# Analysis of Hydroxylamine Glycosidic Linkages: Structural Consequences of the NO Bond in Calicheamicin

**Suzanne Walker,† David Gange,‡ Varsha Gupta,† and Daniel Kahne*,†**

*Contribution from the Department of Chemistry, Princeton University, Princeton, New Jersey 08544, and American Cyanamid Company, Agricultural Research Division, Princeton, New Jersey 08540*

*Received October 19, 1993®*

**Abstract:** The antitumor activity of calicheamicin is related to its ability to bind to and cleave double-stranded DNA. There is substantial evidence that the oligosaccharide-aryl tail of calicheamicin plays a critical role in the binding selectivity. The calicheamicin oligosaccharide contains some unusual structural elements that may be related to the DNA binding function. A better understanding of how structure is related to function in the calicheamicin oligosaccharide could result in an ability to design new DNA binders. In this paper, the influence of the hydroxylamine glycosidic linkage on the shape of the calicheamicin oligosaccharide is analyzed in detail using a combination of experimental data and molecular mechanics calculations. As part of this work, parameters for N–O bonds have been developed for use with the program DISCOVER (AMBER force field). The analysis indicates that the unusual N–O bond in calicheamicin, with its distinctive torsion angle preferences, organizes the two halves of the molecule into a shape that complements the shape of the minor groove.

## Introduction

The activity of many glycosylated antitumor antibiotics is related to their ability to bind to DNA.[1] In several cases it has been shown that the oligosaccharide portions of these antitumor agents play a critical role in DNA binding.[1c-g] There is considerable interest in developing an understanding of the molecular basis for specificity and affinity in the interactions between oligosaccharides and DNA since the result may be an ability to design new DNA binders.

We have been studying the glycosylated antitumor antibiotic calicheamicin $\gamma^1$ (Figure 1), a member of the diyne-ene family of antitumor agents.[2] The diyne-ene antibiotics rearrange to form diradicals that abstract hydrogen atoms from the DNA backbone, initiating DNA strand scission and ultimately causing cell death.[3] The proposed mechanism for DNA damage by calicheamicin is shown in Scheme 1. Calicheamicin is unusual among the diyne-ene antibiotics because it causes double-stranded lesions almost exclusively and is highly site selective, binding to and cleaving TCCT, TCTC, TTTT, and other pyrimidine/purine tracts.[1g,4] There is substantial evidence that the oligosaccharide aryl tail of calicheamicin plays an important role in the binding selectivity.[1d-g,5]

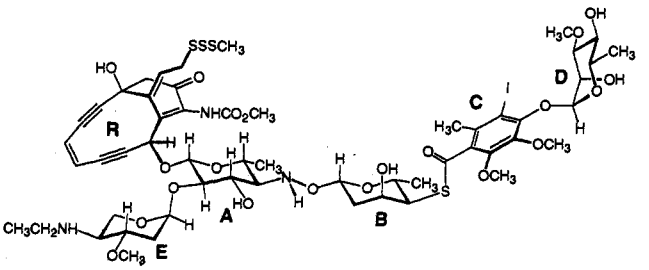


**Figure 1.** Calicheamicin $\gamma^1$.

We would like to understand the structural elements that make the calicheamicin oligosaccharide a good minor groove binder.

The structure of an oligosaccharide depends largely on the glycosidic linkages.[6] Two standard monosaccharides can be linked through a glycosidic bond in many different ways. For example, the stereochemistry at the anomeric center of the glycosyl donor may be either $\alpha$ or $\beta$, and the linkage may be to a primary alcohol (usually the C6 hydroxyl) or to a secondary alcohol on the acceptor. The acceptor alcohol may itself be axial or equatorial depending on the sugar series. Thus, two monosaccharides can combine to produce many disaccharides with very different shapes and properties. An enormous amount of structural work has been done on eukaryotic oligosaccharides in an effort to understand how their torsion angle preferences and flexibility influence various biochemical recognition events.[6] However, prokaryotic oligosaccharides such as calicheamicin have been the subject of much less attention, despite the fact that many of them are components of important therapeutic agents.

From a structural standpoint, the calicheamicin oligosaccharide contains some unusual features. Perhaps the most striking feature is the three-bond hydroxylamine glycosidic linkage which connects monosaccharides A and B (Figure 1). Three-bond glycosidic linkages to C6 primary alcohols are common in oligosaccharides, and they tend to be flexible relative to other linkages.[6] However, this three-bond linkage connects C1 to C4 rather than C1 to C6, and it is through a hydroxylamine rather than a hydroxymethyl spacer. It has been known for a long time that hydroxylamine bonds have unusual conformational preferences. We have

† Princeton University.
‡ American Cyanamid Co.
• Abstract published in *Advance ACS Abstracts*, March 15, 1994.

(1) (a) Gao, X.; Mirau, P.; Patel, D. J. *J. Mol. Biol.* **1992**, *223*, 259. (b) Sastry, M.; Patel, D. J. *Biochemistry* **1993**, *32*, 6588. (c) Silva, D. J.; Goodnow, R.; Kahne, D. *Biochemistry* **1993**, *32*, 463 and references therein. (d) Drak, J.; Iwasawa, N.; Danishefsky, S.; Crothers, D. M. *Proc. Natl. Acad. Sci. U.S.A.* **1991**, *88*, 7464. (e) Aiyar, J.; Danishefsky, S.; Crothers, D. M. *J. Am. Chem. Soc.* **1992**, *114*, 7552. (f) Nicolaou, K. C.; Tsay, S.-C.; Suzuki, T.; Joyce, G. F. *J. Am. Chem. Soc.* **1992**, *114*, 7555. (g) Walker, S.; Landovitz, R.; Ding, W.-D.; Ellestad, G. A.; Kahne, D. *Proc. Natl. Acad. Sci. U.S.A.* **1992**, *89*, 4608. (h) Matsuzawa, Y.; Oki, T.; Takeuchi, T.; Umezawa, H. *J. Antibiot.* **1981**, 1596. (i) Fritzche, H.; Wahnert, U. *Biochemistry* **1987**, *26*, 1996.

(2) Lee, M. D.; Ellestad, G. A.; Borders, D. B. *Acc. Chem. Res.* **1991**, *24*, 235.

(3) (a) Goldberg, I. H. *Acc. Chem. Res.* **1991**, *24*, 191. (b) Sugiura, Y.; Uesawa, Y.; Takahashi, T.; Kuwahara, J.; Golik, J.; Doyle, T. W. *Proc. Natl. Acad. Sci. U.S.A.* **1989**, *86*, 7672. (c) Sugiura, Y.; Matsumoto, T. *Biochemistry* **1993**, *32*, 5548. (d) Zein, N.; Colson, K. L.; Leet, J. E.; Schroeder, D. R.; Solomon, W.; Doyle, T. W.; Casazza, A. M. *Proc. Natl. Acad. Sci. U.S.A.* **1993**, *90*, 2822.

(4) Zein, N.; Sinha, A. M.; McGahren, W. J.; Ellestad, G. A. *Science* **1988**, *240*, 1198.

(5) Walker, S.; Murnick, J.; Kahne, D. *J. Am. Chem. Soc.* **1993**, *115*, 7954.

(6) Meyer, B. In *Topics in Current Chemistry:* Thiem, J., Ed.; Springer-Verlag: Berlin, 1990; Vol. 154, pp 143–208 and references therein.

0002-7863/94/1516-3197$04.50/0 

**Scheme 1.** Proposed Mechanism of DNA Damage by Calicheamicin $\gamma^1$

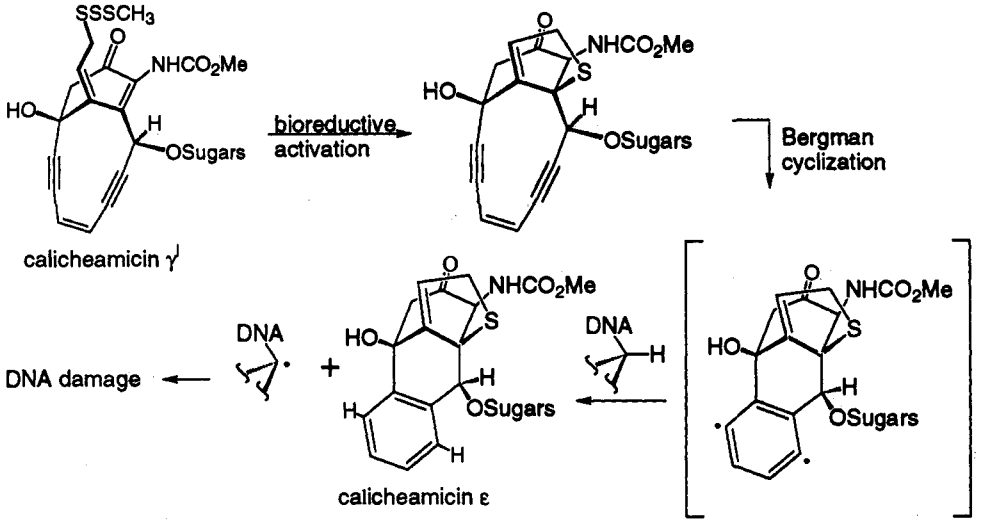


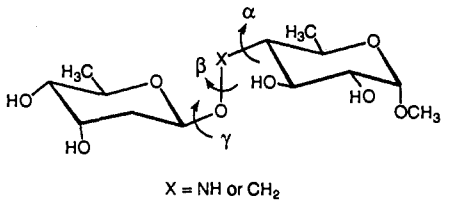


**Figure 2.** Torsion angle labels.

previously suggested that the hydroxylamine glycosidic linkage in calicheamicin may be important for binding because it determines the relative orientation of the two halves of the molecule.[7]

In this paper, we address the influence of the hydroxylamine glycosidic linkage between the A and B sugars on the shape of the calicheamicin oligosaccharide. As part of this effort, we have developed parameters for N–O bonds for use with the program DISCOVER from Biosym (AMBER force field). We have used this force field to study the low-energy conformers around the hydroxylamine glycosidic linkage in model systems. The molecular mechanics results are consistent with experimental data, indicating the validity of the parametrization. NMR data on calicheamicin and a calicheamicin–DNA complex show that the major hydroxylamine conformer identified in solution binds to DNA without undergoing large structural changes. We believe that the N–O bond is critical for good DNA binding because it organizes the calicheamicin oligosaccharide into a shape that complements the shape of the minor groove.

## Experimental Section

**Nomenclature.** To avoid confusion, we did not use the standard carbohydrate nomenclature of $\phi$, $\psi$, and $\omega$ to describe the torsion angles in the unusual three bond glycosidic linkages discussed herein. Instead, the torsion angles are defined as $\alpha$ = C3–C4–X–O, $\beta$ = C4–X–O–C1, and $\gamma$ = X–O–C1–O5, where X is either carbon or nitrogen depending on context (Figure 2).

**Ab Initio Studies.** Computations on hydroxylamine, *N*-methylhydroxylamine, *O*-methylhydroxylamine, and *N*,*O*-dimethylhydroxylamine were performed with the GUASSIAN 90 suite of programs.[8] Hartree–Fock energies and optimized structures were determined with the 6-31G* basis set.[9] Second-order Møller–Plesset (MP2) perturbation theory was used to correct the structures and energies for the effects of electron correlation.[10] Hydroxylamine and *O*-methylhydroxylamine have a plane of symmetry, defined by the N–O–R atoms (R = H or $CH_3$), which bisects the H–N–H angle; these molecules were constrained to maintain $C_s$ symmetry. Stationary points were confirmed to be transition states or minima through the observation of one or zero imaginary frequencies by numeric harmonic vibrational frequency analysis. Enthalpies were computed by correcting total energies for zero-point vibrational energy.

**Parameter Development.** A new atom type was introduced for the hydroxylamine nitrogen. The parameters associated with this new atom type are shown in Table 1. The other atom types that appear in the bond length, bond angle, and torsional parameters were taken from Homans's parameters for carbohydrates in the AMBER force field.[11] The equilibrium bond lengths and bond angles for the hydroxylamine group are based upon microwave data and *ab initio* calculations (*vide supra*), modified as suggested by Allinger (*QCPE Bulletin*).[12-15] Force constants were initially determined by the method of interpolation described by Weiner.[16] The initial force parameters for bond lengths and bond angles were then adjusted to produce the best fit to vibrational frequency data. The torsional parameters were obtained by calculating the rotational barriers in the absence of torsional parameters and then adjusting the torsional parameters to obtain the best fit to the *ab initio* energy barriers. The van der Waals parameter for the hydroxylamine nitrogen was taken to be the same as that for a tertiary amine. No hydrogen bond terms were introduced. Bond angle and torsional parameters for other atom types used in the reported force field calculations were taken directly from Homans, except that explicit torsional parameters for C–C–O–C glycosidic bond torsions were introduced after it was found that including them gave better results. The explicit torsional parameters were developed to reproduce the experimental and *ab initio* data on rotational barriers for methanol and methyl ethyl ether.[17] The C–C–O–C glycosidic bond torsions are given in Table 1 below the NO bond torsional parameters.

**Charges.** A variety of methods have been described for determining suitable partial charges.[18] Attempts to use ESP charges from MOPAC, CHELP, and CHELPG gave unreasonable results for the cases we examined. For our calculations, we found that computing Mulliken

(7) (a) Walker, S.; Valentine, K. G.; Kahne, D. *J. Am. Chem. Soc.* **1990**, *112*, 6428. (b) Walker, S.; Yang, D.; Kahne, D.; Gange, D. *J. Am. Chem. Soc.* **1991**, *113*, 4716.

(8) Frisch, M. J.; Head-Gordon, M.; Trucks, G. W.; Foresman, J. B.; Schlegel, H. B.; Raghavachari, K.; Robb, M.; Binkley, J. S.; Gonzalez, C.; Defrees, D. J.; Fox, D. J.; Whiteside, R. A.; Seeger, R.; Melius, C. F.; Baker, J.; Martin, R. L.; Kahn, L. R.; Stewart, J. J. P.; Topiol, S.; Pople, J. A. *GAUSIAN 90*; Gaussian, Inc.: Pittsburgh, PA, 1990.

(9) Hariharan, P. C.; Pople, J. A. *Theor. Chim. Acta* **1973**, *28*, 213.

(10) Møller, C.; Plesset, M. S. *Phys. Rev.* **1934**, *46*, 618.

(11) Homans, S. W. *Biochemistry* **1990**, *29*, 9110.

(12) Allinger, N. L. *QCPE Bull.*, **1988**, *8*(2) (supplementary enclosure).

(13) (a) Pedersen, L.; Morokuma, K. *J. Chem. Phys.* **1967**, *46*, 3941. (b) Fink, W. H.; Pan, D. C.; Allen, L. C. *J. Chem. Phys.* **1967**, *47*, 358. (c) Radom, L.; Hehre, W. J.; Pople, J. A. *J. Am. Chem. Soc.* **1972**, *94*, 2371. (d) Giguere, P. A.; Liu, I. D. *Can. J. Chem.* **1952**, *30*, 948. (e) Tsunekawa, S. *J. Phys. Soc. Jpn.* **1972**, *33*, 167. (f) Fong, M. Y.; Johnson, L. J.; Harmony, M. D. *J. Mol. Spectrosc.*, **1973**, *54*, 45. (g) Sung, E.-M.; Harmony, M. D. *J. Mol. Spectrosc.* **1979**, *74*, 228. (h) Rankin, D. W. H.; Todd, M. R.; Riddell, F. G.; Turner, E. S. *J. Mol. Struct.*, **1981**, *71*, 171.

(14) Reviews: (a) Riddell, F. G. *Tetrahedron* **1981**, *37*, 849. (b) Raban, M.; Kost, D. *Tetrahedron* **1984**, *40*, 3345.

(15) Full details on the *ab initio* calculations will be reported elsewhere.

(16) Weiner, S. J.; Kollman, P. A.; Case, D. A.; Singh, U. C.; Ghio, C.; Alagona, G.; Profeta, S.; Weider, P. J. *J. Am. Chem. Soc.* **1984**, *106*, 765.

(17) Allinger, N. L.; Rahman, M.; Lii, J.-H. *J. Am. Chem. Soc.* **1990**, *112*, 8293.

**Table 1.** Bond, Angle, and Torsional Parameters for the Various Atom Types Discussed

| atom type (symbols) | mass | type | atom type (symbols) | mass | type | atom type (symbols) | mass | type |
|---|---|---|---|---|---|---|---|---|
| CS | 12.0000 | $sp^3$ carbon | BH | 1.007 825 | $\beta$ anomeric hydrogen | OA | 15.994 91 | $\alpha$ anomeric oxygen |
| AC | 12.0000 | $\alpha$ anomeric carbon | HY | 1.007 825 | hydroxyl hydrogen | OB | 15.991 91 | $\beta$ anomeric oxygen |
| BC | 12.0000 | $\beta$ anomeric carbon | O | 15.994 91 | carbonyl oxygen | OE | 15.994 91 | ring oxygen |
| AH | 1.007 825 | $\alpha$ anomeric hydrogen | OT | 15.994 91 | hydroxyl oxygen | NO | 14.003 07 | hydroxylamine oxygen |
| HT | 1.007 825 | $sp^3$ hydrogen | | | | | | |

| bond type | $K_f$ | $r_e$ | bond type | $K_f$ | $r_e$ | bond type | $K_f$ | $r_e$ |
|---|---|---|---|---|---|---|---|---|
| NO OA | 337.0 | 1.462 | NO HY | 440.0 | 1.010 | NO CS | 367.0 | 1.471 |
| NO OB | 337.0 | 1.462 | | | | | | |

| angle type | $K_t$ | $t_e$ | angle type | $K_t$ | $t_e$ | angle type | $K_t$ | $t_e$ |
|---|---|---|---|---|---|---|---|---|
| HY NO HY | 45.0 | 107.23 | NO OA AC | 70.0 | 109.97 | CS NO OB | 90.0 | 105.27 |
| HY NO OA | 48.5 | 103.50 | NO OB OC | 70.0 | 109.97 | HT CS NO | 45.9 | 109.89 |
| HY NO OB | 48.5 | 193.50 | NO OA CS | 70.0 | 109.97 | CS CS NO | 80.0 | 109.70 |
| NO OA HY | 60.0 | 101.39 | NO OB CS | 70.0 | 109.97 | CS NO HY | 35.0 | 108.30 |
| NO OB HY | 60.0 | 101.39 | CS NO OA | 90.0 | 105.27 | | | |

| torsion type | $K_n$ | $n$ | $\gamma$ | torsion type | $K_n$ | $n$ | $\gamma$ |
|---|---|---|---|---|---|---|---|
| OE AC OA NO | 2.150 | 1.0 | 300.0 | CS NO OB HY | 1.100 | 1.0 | 0.0 |
| | | | | | 2.800 | 2.0 | 0.0 |
| AH AC OA NO | 1.750 | 2.0 | 60.0 | CS NO OA AC | 1.900 | 1.0 | 0.0 |
| | | | | | 2.900 | 2.0 | 0.0 |
| CS AC OA NO | 0.850 | 3.0 | 0.0 | CS NO OB BC | 1.900 | 1.0 | 0.0 |
| | | | | | 2.900 | 2.0 | 0.0 |
| OE BC OB NO | −1.050 | 1.0 | 0.0 | CS NO OA CS | 1.900 | 1.0 | 0.0 |
| | | | | | 2.900 | 2.0 | 0.0 |
| BH BC OB NO | 1.250 | 2.0 | 240.0 | CS NO OB CS | 1.900 | 1.0 | 0.0 |
| | | | | | 2.900 | 2.0 | 0.0 |
| CS BC OB NO | 1.400 | 3.0 | 0.0 | HT CS NO HY | 0.120 | 3.0 | 0.0 |
| HY NO OA HY | 2.600 | 1.0 | 0.0 | HT CS NO OA | 0.450 | 3.0 | 0.0 |
| | 2.700 | 2.0 | 0.0 | | | | |
| HY NO OB HY | 2.600 | 1.0 | 0.0 | HT CS NO OB | 0.450 | 3.0 | 0.0 |
| | 2.700 | 2.0 | 0.0 | | | | |
| HY NO OA CS | 1.400 | 1.0 | 0.0 | CS CS NO HY | 0.200 | 3.0 | 0.0 |
| | 2.800 | 2.0 | 0.0 | | | | 0.0 |
| HY NO OB CS | 1.400 | 1.0 | 0.0 | HY NO OB BC | 1.400 | 1.0 | 0.0 |
| | 2.800 | 2.0 | 0.0 | | 2.800 | 2.0 | 0.0 |
| NO OA CS HT | 0.370 | 3.0 | 0.0 | HY NO OA AC | 1.400 | 1.0 | 0.0 |
| | | | | | 2.800 | 2.0 | 0.0 |
| NO OB CS HT | 0.370 | 3.0 | 0.0 | CS CS OT CS | 0.700 | 1.0 | 0.0 |
| | | | | | 0.900 | 3.0 | 0.0 |
| CS NO OA HY | 1.100 | 1.0 | 0.0 | CS CS OA AC | 0.700 | 1.0 | 0.0 |
| | 2.800 | 2.0 | 0.0 | | 0.900 | 3.0 | 0.0 |
| * CS NO * | 1.021 | 3.0 | 0.0 | CS CS OB BC | 0.700 | 1.0 | 0.0 |
| | | | | | 0.900 | 3.0 | 0.0 |
| * CS OA * | 0.443 | 3.0 | 0.0 | * CS OB * | 0.443 | 3.0 | 0.0 |

| van der Waals terms | $r^*$ | $e$ |
|---|---|---|
| NO- | 3.70 | −0.1200 |

charges on a reasonable starting structure by the MNDO method contained in the program MOPAC (QCPE 455) gave good results. The magnitude of the charges obtained is similar to the magnitude of the average charges used by Homans.

**Minimizations and Simulations.** All calculations were performed using the AMBER force field as contained within the program DISCOVER (Version 2.8, Biosym Technologies Inc.) but modified to contain the Homans parameters for carbohydrates and the hydroxylamine parameters reported herein.[11] Simulated structures were created with INSIGHTII, a graphics program designed to work with the DISCOVER package. A distance-dependent dielectric ($1/r$) was used in the minimizations, and 1–4 interactions were scaled by a factor of 0.5. All structures were minimized until the maximum derivative was less than $1 \times 10^{-6}$ kcal/Å.

**Grid Searches.** Grid searches were performed by rotating bonds in 30° increments to generate a family of starting conformations differing only in the torsions around the glycosidic bonds. A 100 kcal/rad forcing potential was then applied to hold the glycosidic bonds at the desired angles, and each conformation was separately minimized until the derivative was less than $1 \times 10^{-6}$ kcal/Å. This grid searching procedure permits the sugars to relax as the glycosidic bonds are rotated, generating a more realistic contour map than a rigid rotor treatment, which seriously overestimates the conformational energies near rotational transition states. In addition, minimizing each structure separately avoids the hysteresis effects produced by using a previous conformational minimum as the starting point for the next minimization in the grid search.[19]

**Syntheses.** Room temperature and variable temperature $^1$H NMR spectra were recorded on a Jeol GSX-500 MHz spectrometer unless otherwise specified. Room temperature $^{13}$C NMR spectra were recorded on a JEOL GSX 270-MHz spectrometer at 67.5 MHz unless otherwise specified.

**4-Methoxyamino Monosaccharide 1.** To a solution of sugar triflate **6A** (0.095 g, 1.0 equiv) in 2.5 mL of dry DMF was added 5 mL of distilled methoxyamine (Scheme 2). The reaction mixture was stirred at 25 °C for 3 h, after which the excess solvent was removed under reduced pressure. The residue obtained was stirred with 10 mL of 1% NaOH in methanol/$H_2O$ (20:1) at 25 °C for 1 h. The reaction mixture was neutralized with

(18) (a) Cox, S. R.; Williams, D. E. *J. Comput. Chem.* **1981**, *2*, 304. (b) Chirlian, L. E.; Francl, M. M. *J. Comput. Chem.* **1987**, *8*, 894. (c) Breneman, C. M.; Wiberg, K. B. *J. Comput. Chem.* **1990**, *11*, 361. (d) Besler, B. H.; Merz, K. M.; Kollman, P. A. *J. Comput. Chem.* **1990**, *11*, 431. (e) Stouch, T. R.; Williams. D. E. *J. Comput. Chem.* **1993**, *14*, 858.

(19) French, A. D.; Brady, J. W., Eds. *Computer Modeling of Carbohydrate Molecules*; American Chemical Society: Washington, DC, 1990.

**Scheme 2.** Synthesis of Monosaccharide Model Systems[a]

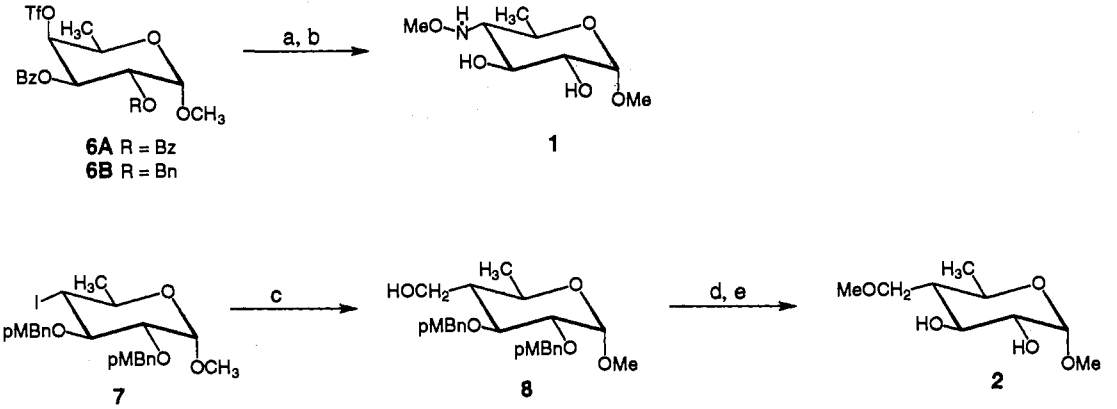

[a] (a) $MeONH_2$:DMF (2:1), 25 °C, 3 h, 89%; (b) 1% NaOH, $CH_3OH$, 25 °C, 1 h, 92%; (c) 0.1 equiv of $Ph_3GeH$, 0.1 equiv of AIBN, 2 equiv of $NaBH_3CN$, benzene, 105 °C, 12 h, 35%; (d) 2 equiv of NaH, 4 equiv of $CH_3I$, THF, 40 °C, 1 h, 90%; (e) 2.5 equiv of DDQ, $CH_2Cl_2$:$H_2O$ (20:1), 25 °C, 1 h, 63%.

**Scheme 3.** Synthesis of Disaccharide Model Systems[a]

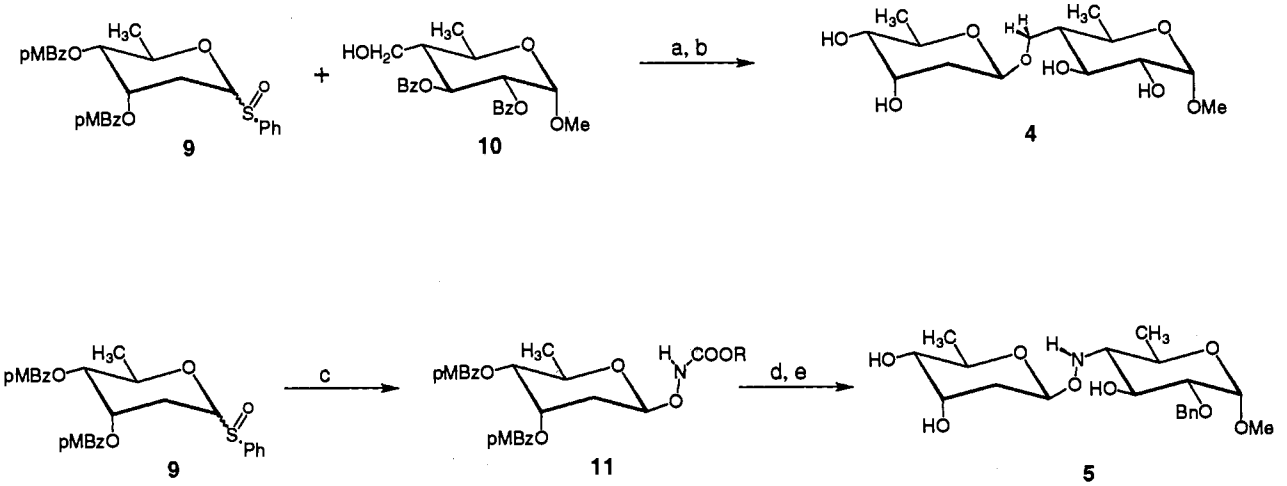

[a] (a) 1 equiv of $Tf_2O$, 1.2 equiv of 2,6-di-*tert*-butyl-4-methylpyridine, $Et_2O$:$CH_2Cl_2$ (1:2), –78 °C, 0.5 h; (b) NaOH, $CH_3OH$:$H_2O$ (30:1), 25 °C, 1 h, 38%; (c) HONHCOOEt, 1.1 equiv of $Tf_2O$, 2 equiv of 2,6-di-*tert*-butyl-4-methylpyridine, $CH_2Cl_2$, –60 °C, 1 h, 38%; (d) 2 equiv of NaH, $Et_2O$:HMPA (3:1), **5B**, –24 °C, (e) NaOH, $CH_3OH$:EtOH, 25 °C, 62%, 1 h.

0.5 N hydrochloric acid (5 mL) and extracted with ethyl acetate (3 × 25 mL). The combined ethyl acetate fractions were dried over anhydrous sodium sulfate, and solvent was removed under reduced pressure. The residue obtained was purified by flash chromatography (80/20 ethyl acetate/petroleum ether) to afford monosaccharide **1** in 81% yield: $^1$H NMR ($CD_3OD$) $\delta$ 4.59 (1H, d, $J$ = 3.90 Hz, $H_1$), 3.88 (1H, dq, $J$ = 9.77, 6.25 Hz, $H_5$), 3.82 (1H, dd, $J$ = 9.78, 9.76 Hz, $H_3$), 3.47 (3H, s, $OCH_3$), 3.38 (1H, dd, $J$ = 9.58, 3.72 Hz, $H_2$), 3.36 (3H, s, $OCH_3$), 2.22 (1H, dd, $J$ = 9.97, 9.76 Hz, $H_4$), 1.29 (3H, d, $J$ = 6.25 Hz, $H_6$); $^{13}$C NMR ($CD_3OD$) $\delta$ 101.35, 74.71, 69.47, 68.72, 66.50, 62.30, 55.46, 18.95; HRMS for $C_8H_{17}NO_5$ ($M^+$) calcd 207.1107, found 207.1112.

**4-Methoxymethyl Monosaccharide 2.** According to our previously published procedure,[20] a solution of sugar iodide **7** (0.250 g, 1.0 equiv), triphenylgermane (0.018 g, 0.1 equiv), $NaBH_3CN$ (0.061 g, 2.0 equiv), and AIBN (0.008 g, 0.1 equiv) in 26 mL of benzene/THF (20:1) was taken in a glass tube and inserted in a 300-mL autoclave. The solution was degassed and then stirred at 105 °C under 1400 psi of CO. After 12 h, the reaction was cooled to room temperature, and CO was released slowly. The hydroxymethyl monosaccharide **8** was isolated after aqueous workup and purification by flash chromatography (25/75 ethyl acetate/petroleum ether). To a solution of monosaccharide **8** in 10 mL of THF were added NaH (0.003 g, 2 equiv), and $CH_3I$ (0.014 mL, 4 equiv). The reaction mixture was stirred at 40 °C for 1 h. The reaction was then quenched with water, extracted with ethyl acetate (2 × 10 mL), dried over $Na_2SO_4$, and concentrated. To a solution of the crude product in 10 mL of $CH_2Cl_2$/$H_2O$ (20:1) was added DDQ (0.006 g, 2.5 equiv). After 1 h of being stirred at room temperature, the reaction mixture was filtered through Celite, and the filtrate was concentrated. The desired monosaccharide **2** was isolated after purification by flash chromatography (70/30 ethyl acetate/petroleum ether) in 25% yield: $^1$H NMR ($CD_3OD$) $\delta$ 4.51 (1H, d, $J$ = 3.63 Hz, $H_1$), 3.77 (1H, dq, $J$ = 10.23, 6.27 Hz, $H_5$), 3.62 (1H, dd, $J$ = 10.23, 9.90 Hz, $H_3$), 3.54 (1H, dd, $J$ = 9.89, 3.63 Hz, $H_7$), 3.35 (1H, dd, $J$ = 9.90, 2.64 Hz, $H_7$), 3.26 (3H, s, $OCH_3$), 3.25 (1H, dd, $J$ = 9.56, 3.63 Hz, $H_2$), 3.20 (3H, s, $OCH_3$), 1.20 (1H, dddd, $J$ = 10.56, 10.23, 3.30, 2.97 Hz, $H_4$), 1.10 (3H, d, J = 6.27 Hz, $H_6$). $^{13}$C NMR ($CD_3OD$) 101.54, 75.31, 70.18, 69.23, 66.61, 55.33, 51.37, 49.71, 19.07; HRMS for $C_8H_{15}O_4$ ($M^+$ – $OCH_3$) calcd 175.0991, found 175.0985.

**Hydroxymethyl-Linked Disaccharide 4.** To a solution of 2,6-dideoxy 3,4-*O*-bis(4-methoxybenzoyl)allose sulfoxide **9** (0.084 g, 1.1 equiv) and 2,6-di-*tert*-butyl-4-methylpyridine (0.056 g, 2.0 equiv) in 15 mL of $CH_2Cl_2$/$Et_2O$(2:1) at –78 °C was added triflic anhydride (0.023 mL, 1.0 equiv) dropwise (Scheme 3). After 15 min, methyl 4,6-dideoxy-2,3-*O*-dibenzoyl-4-(hydroxymethyl)glucoside (**10**) (0.055 g, 1.0 equiv)[20] was added in 1 mL of $CH_2Cl_2$. The reaction mixture was slowly warmed to –35 °C over a period of 1 h.[21] The reaction was then quenched with saturated sodium bicarbonate solution, extracted with $CH_2Cl_2$ (3 × 25 mL), dried over anhydrous $Na_2SO_4$, and concentrated. The crude product obtained was purified by flash chromatography.[22] The disaccharide ($\beta$ anomer) obtained was stirred for 1 h with 1% NaOH in methanol. The reaction mixture was neutralized using 0.5 N HCl solution (5 mL) and extracted with ethyl acetate (2 × 25 mL). The combined ethyl acetate

(20) Gupta, V.; Kahne, D. *Tetrahedron Lett.* **1993**, *34*, 591.

(21) Yang, D.; Kim, S. H.; Kahne, D. *J. Am. Chem. Soc.* **1991**, *113*, 4715.

(22) Kahne, D.; Walker, S.; Cheng, Y.; Van Engen, D. *J. Am. Chem. Soc.* **1989**, *111*, 6881.

fractions were dried over anhydrous $Na_2SO_4$, and the solvent was removed by rotary evaporation. The residue was purified by flash chromatography (80/20 ethyl acetate/petroleum ether) to afford disaccharide **4** in 38% yield. $^1$H NMR ($CD_3OD$) $\delta$ 4.66 (1H, dd, $J$ = 9.52, 1.83 Hz, $H_{1B}$), 4.50 (1H, d, $J$ = 3.66 Hz, $H_{1A}$), 3.95 (1H, dd, $J$ = 10.26, 3.67 Hz, $H_{7A}$), 3.90 (1H, dd, $J$ = 9.53, 3.30 Hz, $H_{3B}$), 3.71 (1H, dq, $J$ = 10.26, 6.23 Hz, $H_{5A}$), 3.61 (1H, dq, $J$ = 10.26, 6.23 Hz, $H_{5B}$), 3.59 (1H, dd, $J$ = 10.26, 9.89 Hz, $H_{3A}$), 3.43 (1H, dd, $J$.= 10.26, 2.56 Hz, $H_{7A}$), 3.26 (1H, dd, $J$ = 9.57, 3.67 Hz, $H_{2A}$), 3.23 (3H, s, $OCH_3$), 3.04 (1H, dd, $J$ = 9.53, 2.93 Hz, $H_{4B}$), 1.84 (1H, ddd, $J$ = 13.55, 3.30, 2.19 Hz, $H_{2B}$), 1.52 (1H, ddd, $J$ = 13.56, 9.89, 2.93 Hz, $H_{2B}$), 1.20 (1H, tdd, $J$ = 10.26, 3.30, 2.93 Hz, $H_{4A}$), 1.12 (3H, d, $J$ = 6.23 Hz, $H_{6A}$), 1.09 (3H, d, $J$ = 6.59 Hz, $H_{6B}$); $^{13}$C NMR ($CD_3OD$) $\delta$ 101.48, 99.58, 74.95, 74.37, 70.94, 69.06, 68.95, 66.75, 55.38, 51.29, 49.76, 39.19, 14.06, 13.01; HRMS for $C_{14}H_{26}O_8$ ($M^+ + Na^+$), calcd 345.1525, found 345.1527.

**Hydroxylamine-Linked Disaccharide 5.** To a solution of 2,6-dideoxy 3,4-*O*-bis(4-methoxybenzoyl)allose sulfoxide **9** (0.057 g, 1.0 equiv) and 2,6-di-*tert*-butyl-4-methylpyridine (0.056 g, 2.0 equiv) in 5 mL of $CH_2Cl_2$ at −78 °C was added triflic anhydride (0.025 mL, 1.1 equiv). After 10 min, $HONHCOOC_2H_5$ (0.043 g, 3.0 equiv) in 1 mL of $CH_2Cl_2$ was added dropwise.[22] The reaction was slowly warmed to 25 °C over a period of 1 h. The reaction was then quenched with saturated $NaHCO_3$, extracted with $CH_2Cl_2$ (2 × 10 mL), dried over anhydrous $Na_2SO_4$, and concentrated. The crude product obtained was purified by flash chromatography (35/65 ethyl acetate/petroleum ether) to obtain glycosyl urethane **11**. To a solution of **11** (0.014 g, 1.0 equiv) in 5 mL of $Et_2O$ at −24 °C was added excess NaH (0.010 g). After complete deprotonation, HMPA (2 mL) was added, and the suspension was stirred vigorously. A solution of sugar triflate **6B** (0.015, 1.2 equiv) in 1 mL of $Et_2O$ was added dropwise, and the reaction flask was slowly warmed to −0.5 °C over a period of 1 h. The reaction was then quenched with saturated $NH_4Cl$ solution and extracted with $CH_2Cl_2$ (2 × 10 mL). The combined $CH_2Cl_2$ fractions were dried over anhydrous $Na_2SO_4$, filtered, and concentrated. The crude product obtained was stirred with 5 mL of 1% NaOH in $CH_3OH/H_2O$ (20:1) for 1 h at 25 °C. The reaction was then quenched with 5 mL of 0.5 N HCl solution, extracted with ethyl acetate (3 × 10 mL), dried over anhydrous $Na_2SO_4$, and concentrated. The desired disaccharide **5** was isolated by flash chromatography (50% ethyl acetate, petroleum ether) in 26% yield: $^1$H NMR ($CD_3OD$) $\delta$ 7.3–7.4 (5H, m, $H_{aromatic}$), 4.96 (1H, dd, $J$ = 10.00, 1.90 Hz, $H_{1B}$), 4.75 (1H, d, $J_{AB}$ = 11.90 Hz), 4.63 (1H, d, $J_{AB}$ = 12.14 Hz), 4.56 (1H, d, $J$ = 3.57 Hz, $H_{1A}$), 4.10 (1H, t, $J$ = 9.56 Hz, $H_{3A}$), 3.99 (1H, dd, $J$ = 6.42, 3.09 Hz, $H_{3B}$), 3.89 (1H, dq, $J$ = 9.28, 6.19 Hz, $H_5$), 3.76 (1H, dq, $J$ = 9.29, 6.43 Hz, $H_5$), 3.31 (1H, dd, $J$ = 9.76, 3.57 Hz, $H_{2A}$), 3.30 (3H, s, $OCH_3$), 3.12 (1H, dd, $J$ = 9.52, 2.09 Hz, $H_{4B}$), 2.20 (1H, t, $J$ = 10.00 Hz, $H_{4A}$), 1.91 (1H, ddd, $J$ = 13.57, 3.57, 2.14 Hz, $H_{2B}$), 1.60 (1H, ddd, $J$ = 13.33, 10.24, 2.86 Hz, $H_{2B}$), 1.26 (3H, d, $J$ = 6.33 Hz, $H_6$), 1.25 (3H, d, $J$ = 6.19 Hz, $H_6$); $^{13}$C NMR ($CDCl_3$, 67.5 MHz) $\delta$ 129.0, 128.6, 128.4, 100.4, 98.7, 80.8, 73.7, 73.5, 69.9, 68.8, 68.5, 67.3, 64.6, 55.8, 36.2, 18.6; HRMS for $C_{20}H_{31}O_8N$ ($M^+$), calcd 413.2049, found 413.2071.

## Results and Discussion

Nuclear magnetic resonance spectroscopy is frequently used to obtain information on glycosidic linkage conformations in solution. Unfortunately, the preferred conformation(s) around a glycosidic linkage cannot be determined using NMR data alone because there are not enough restraints to lead to a unique structure (or family of structures).[6] For this reason, potential energy calculations are typically used in conjunction with experimental data to analyze oligosaccharide conformation.[6,11,19] Several force fields suitable to treat standard carbohydrates are available.[6,11,19] However, we found that no force fields contained parameters for N–O bonds. Therefore, our first goal when we began this work was to develop parameters for N–O bonds for use in a suitable force field.

**Force Field Parametrization.** The structures of hydroxylamine and various methylated derivatives were studied in the 1960s and 1970s using both experimental methods and *ab initio* calculations.[13,14] It was shown that hydroxylamine has a two-fold rotational barrier and that there is a significant energy difference between the two ground-state conformers. In both conformers, the lone pairs on adjacent atoms are as close to orthogonal as permitted by the bond angles in order to avoid destabilizing orbital interactions. The global minimum conformer has the bonds eclipsing the lone pairs. The other conformer has its bonds staggered (Figure 3). However, the various studies disagreed with regard to the energy difference between hydroxylamine conformers, the height of the rotational barriers, and the influence of substituents on both the rotational profile and the structure of the conformers. In order to develop force field parameters for N–O bonds, we had to resolve some of the discrepancies uncovered in the search for data on hydroxylamine bonds. We carried out *ab initio* calculations on hydroxylamine and some of its methylated derivatives (*N*-methyl-, *O*-methyl-, and *N,O*-dimethylhydroxylamine) at the MP2/6–31G*//MP2/6–31G* level.[15] The *ab initio* results are summarized in Table 2. The *ab initio* results generally agree with the results from earlier studies, although the rotational barrier heights are significantly lower and the energy differences between conformers are smaller than previously calculated by 1.5–4.5 kcal/mol.[13a–c] As expected, substituents have some effect on the energy differences between N–O bond conformers, but the eclipsed conformer is much lower in energy than the staggered conformer in all cases.[23]

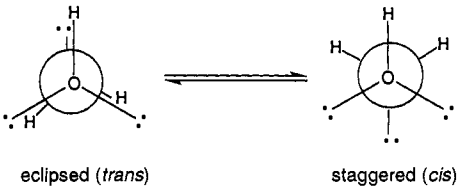


**Figure 3.** Conformers of hydroxylamine.

**Table 2.** $\Delta H_{rel}$ (kcal/mol), *ab Initio* Calculations

| | eclipsed | staggered | rotation 1 | rotation 2 |
|---|---|---|---|---|
| $H_2NOH$ | 0 | 5.95 | 8.05 | |
| MeNHOH | 0 | 4.50 | 7.86 (H–H) | 7.29 (H–Me) |
| $H_2NOMe$ | 0 | 3.40 | 6.30 | |
| MeNHOMe | 0 | 4.60 | 6.18 (H–Me) | 11.95 (Me–Me) |

**Table 3.** $\Delta H_{rel}$ (kcal/mol), Molecular Mechanics Calculations

| | eclipsed | staggered | rotation 1 | rotation 2 |
|---|---|---|---|---|
| $H_2NOH$ | 0 | 6.10 | 8.11 | |
| MeNHOH | 0 | 4.47 | 8.51 (H–H) | 6.59 (H–Me) |
| $H_2NOMe$ | 0 | 3.44 | 6.35 | |
| MeNHOMe | 0 | 4.63 | 6.57 (H–Me) | 11.52 (Me–Me) |

The *ab initio* results were used in conjunction with experimental data on N–O bond lengths and angles to parametrize the AMBER force field contained within the INSIGHTII/DISCOVER package available from Biosym. This force field was originally developed by Kollman and co-workers for use with proteins and nucleic acids and was recently modified by Homans to include parameters for carbohydrates.[11,16] It is an appealing force field for our purposes since it contains parameters for carbohydrates and can be used to model both calicheamicin and the calicheamicin–DNA complex with few additional modifications. The parameters for N–O bonds are shown in Table 1.[24] Torsional profiles for hydroxylamine and its methylated derivatives were calculated using the parametrized force field, and the results are summarized in Table 3. (Details on the calculations are given in the Experimental Section.) There is good agreement with the *ab initio* results (compare Tables 2 and 3). The force field also reproduces the infrared spectrum of hydroxylamine with a root mean square deviation for the peaks of 16 cm$^{-1}$.

(23) Gange, D.; Kallel, E. A. *J. Chem. Soc., Chem. Commun.* **1992**, *11*, 824.

(24) Table 2 also includes explicit torsional parameters for C–O glycosidic bonds. Although Homans and others have argued that the torsional preferences about CCOC glycosidic bonds (the $\psi$ angle in carbohydrate nomenclature) can be adequately simulated without explicitly including torsional terms,[11] we have obtained better results with explicit parameters that produce a better fit between the molecular mechanics torsional profile for $CH_3CH_2OCH_3$ and experimental results.

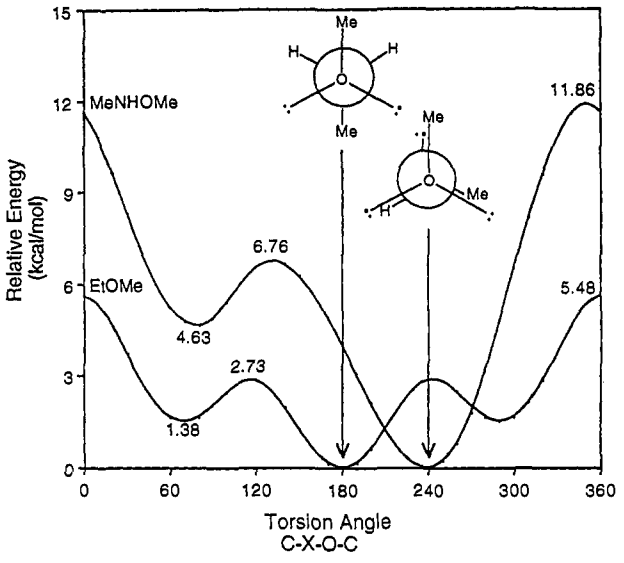


**Figure 4.** (A) Rotational profile for MeNHOMe. (B) Rotational profile for $MeCH_2OMe$.

Figure 4 illustrates the molecular mechanical rotational profile for *N,O*-dimethylhydroxylamine. The rotational profile for methyl ethyl ether, the C–O analogue of *N,O*-dimethylhydroxylamine, is also shown in Figure 4 to highlight the difference between N–O bonds and the C–O bonds more commonly found in three-bond glycosidic linkages. The potential energy surface for the C–O bond analogue is shallow, reflecting the flexibility of hydroxymethyl linkages. In contrast, the hydroxylamine bond is much more rigid; the energy rises steeply as a function of deviations from the preferred conformation. Moreover, the minimum energy conformer for the hydroxylamine derivative corresponds to a transition state for the C–O bond analogue. Thus, the rotational profile for NO bonds suggests that the hydroxylamine glycosidic linkage in calicheamicin must restrict the oligosaccharide to regions of conformational space which would never be occupied in a more typical oligosaccharide.

**Calculations on Monosaccharides.** The modified force field was used to identify the low-energy conformers of a simple model system for the A sugar of calicheamicin and its isosteric C–O analogue (Figure 5). To carry out the calculations, we had to deal with the issue of nitrogen inversion and the fact that in a disubstituted hydroxylamine, where either of the substituents is chiral, there are actually *two* energetically distinct eclipsed (*trans*) conformers (diastereoisomers) around the N–O bond rather than one. The two eclipsed diastereoisomers interconvert by a stepwise process involving both inversion and rotation. (Studies on the interconversion of hydroxylamine conformers have been reviewed by Raban and Kost.[12]) We ultimately decided to carry out grid searches around the $\alpha$ and $\beta$ bonds (see Figure 2 and Experimental Section) of both possible invertomers around nitrogen as well as the CO analogue (**1A**, **1B**, and **2**, Figure 5). Contour plots showing the results of the calculations on the two NO bond isomers **1A** and **1B** and the CO analogue **2** are given in Figure 5.

The $\beta$ angles for **1A**, **1B**, and **2** are approximately −120°, +120°, and 180°, respectively. Each monosaccharide has three conformational minima along the $\alpha$ angle. The major conformer for all three monosaccharides has an $\alpha$ torsion angle of approximately −60°, which places the C4 hydrogen and the exocyclic oxygen in an anti orientation. This is apparently the least hindered conformation. There are secondary minima at approximately 60° and 160°. Thus, **1A**, **1B**, and **2** differ primarily in the $\beta$ angle. The preferred $\alpha$ angles are not significantly affected by the differences in the $\beta$ angles.

The contour plot for the CO analogue shows that more than 50% of the potential energy surface is within 5 kcal/mol of the global minimum, consistent with the high degree of torsional flexibility around the $\beta$ angle. The contour plots for the NO bond isomers show that less than 25% of the potential energy surface is within 5 kcal/mol of the minimum because the NO bond is much more rigid with regard to rotation than the isosteric CO bond.

**Experimental Data on Monosaccharides.** To assess the results of the calculations, we looked at monosaccharides **1** and **2** by NMR. The coupling constants indicate that both the N–O and C–O monosaccharides are fixed in the $^4C_1$ conformation as expected (see Experimental Section).[25] The $\alpha$ angle in monosaccharide **2** can be established readily from the coupling constants between the C4 hydrogen and the exocyclic methylene protons.[26] Both couplings are small, indicating that both methylene hydrogens are gauche to C4, which is consistent with the calculated global minimum conformation. The $\alpha$ angle in the N–O bond compound cannot be determined readily by NMR because there is only one proton on the nitrogen, and one coupling is not sufficient to fix the angle. Moreover, the nitrogen inverts, so there are six rather than three possible staggered conformations. Nevertheless, in acetone, a solvent in which hydrogen exchange is suppressed, the NH proton appears as a sharp singlet, indicating a small coupling consistent with an average conformation in which the hydroxylamine hydrogen is gauche to the C4 hydrogen.

The calculations suggest that both invertomers at nitrogen of monosaccharide **1** are represented in solution. Although variable temperature NMR studies are not normally of use in studying torsion angle preferences in oligosaccharides because the barriers to bond rotation are too low, hydroxylamines have unusually high barriers to interconversion.[13,14] This means that it is possible to use dynamic NMR to determine whether both nitrogen invertomers (**1A** and **1B**) are actually present in solution. NMR spectra of compound **1** in $CD_3OD$ at different temperatures are shown in Figure 6. As the temperature decreases, the resonance lines broaden and eventually decoalesce. At very low temperatures, two sets of peaks representing the two different nitrogen invertomers can be frozen out. The relative energies of the conformers can be determined from the relative populations. In the case of compound **1**, the two NO bond isomers are approximately equal in energy (the population ratio is about 1.5:1 at the low-temperature limit).

The NMR data on the monosaccharides confirm the calculations in two key respects. First, the calculations predict that the C4 hydrogen and the exocyclic oxygen are anti to one another in the lowest energy conformations of compounds **1A**, **1B**, and **2**. The calculations suggest that this conformation is more stable than that of any other conformer for steric reasons. The NMR data establish that this is the *only* significantly populated conformer for compound **2**. The NMR data on compound **1**, although less informative, are also consistent with an average conformation in which the oxygen is anti to the C4 hydrogen and the NH hydrogen is gauche to the C4 hydrogen. Taken together, the experimental data strongly suggest that the −60° $\alpha$ torsion is heavily preferred for *both* the NO and the CO bond compounds. The experiments also confirm that the relative energies of the two nitrogen invertomers are very close in energy, as predicted by the force field calculations. As shown below, the energy difference between nitrogen invertomers increases when the substituent on the hydroxylamine oxygen becomes bulkier.

**Calculations on Disaccharides.** Although the studies on the monosaccharides were a useful starting point for assessing the parametrization, we wanted a model system that more closely approximates the hydroxylamine glycosidic linkage in caliche-

(25) Binkley, R. W. *Modern Carbohydrate Chemistry*; Marcel Dekker, Inc.: New York, 1988; pp 47–74.

(26) Kishi and co-workers have established the utility of C-glycosides as glycosidic bonds of carbohydrates in the absence of electronic stabilization. Our C–O bond analogue serves a similar purpose in the conformational analysis of the $\alpha$ angle in these unusual systems. See: Goekjian, P. G.; Wu, T.-C.; Kishi, Y. *J. Org. Chem.* **1991**, *56*, 6412.

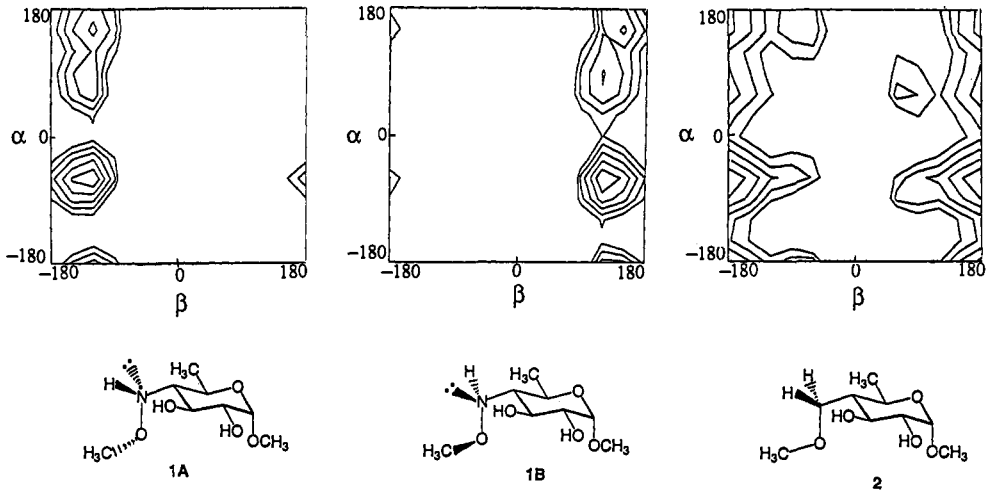


**Figure 5.** Contour plots representing the potential energy surface for model monosaccharides **1** and **2**.

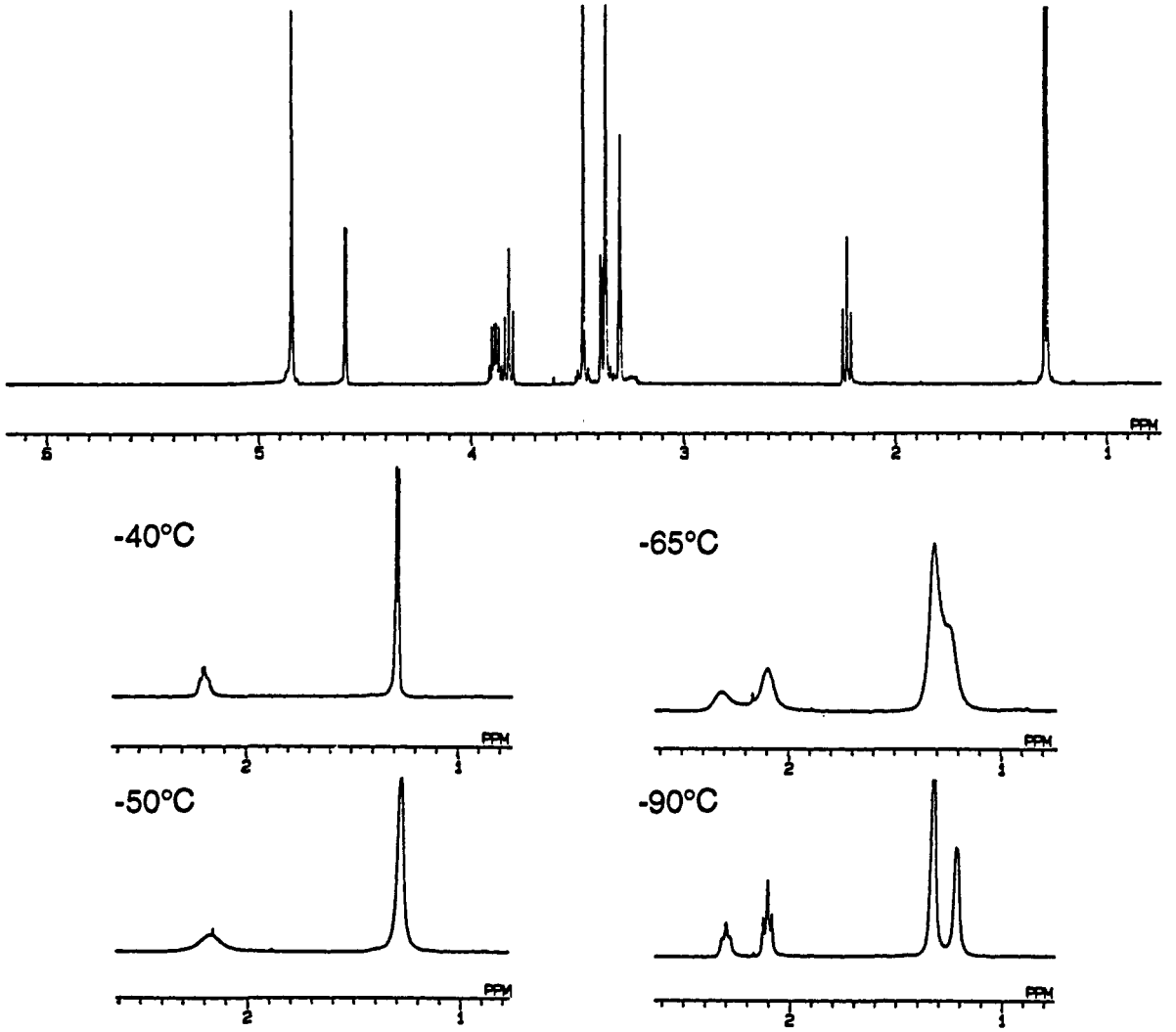


**Figure 6.** NMR spectra ($CD_3OD$) for the A6 methyl and A4 hydrogen of monosaccharide **1** at various temperatures.

amicin $\gamma^1$. Accordingly, we carried out force field calculations on both nitrogen invertomers of disaccharide **3** and its CO analogue **4** (Figure 7). Disaccharide **3** is a model system for the A–B disaccharide in calicheamicin. Contour plots showing the occupied regions of conformational space around the $\alpha$ and $\beta$ angles and the $\alpha$ and $\gamma$ angles of both NO bond isomers of disaccharide **3** (**3A** and **3B**) and of disaccharide **4** are shown in Figure 7. The preferred $\alpha$, $\beta$, and $\gamma$ torsion angles of the low-energy conformers are given in Table 4. The preferred $\alpha$ and $\gamma$ angles are essentially identical for all three disaccharides. The global minimum for all three conformers has an $\alpha$ angle of approximately $-60°$ and a $\gamma$ angle of approximately 170°. The $\beta$ angles for **3A**, **3B** and **4** are approximately $-120°$, $+120°$, and 180°. As in the monosaccharide case, there are secondary minima for all three disaccharides at approximately 60° and 160° for the $\alpha$ angle. There is also a secondary minimum at $\gamma = -60°$ (approximately) for each disaccharide. Thus, as the contour plots demonstrate, the differences between the two nitrogen invertomers

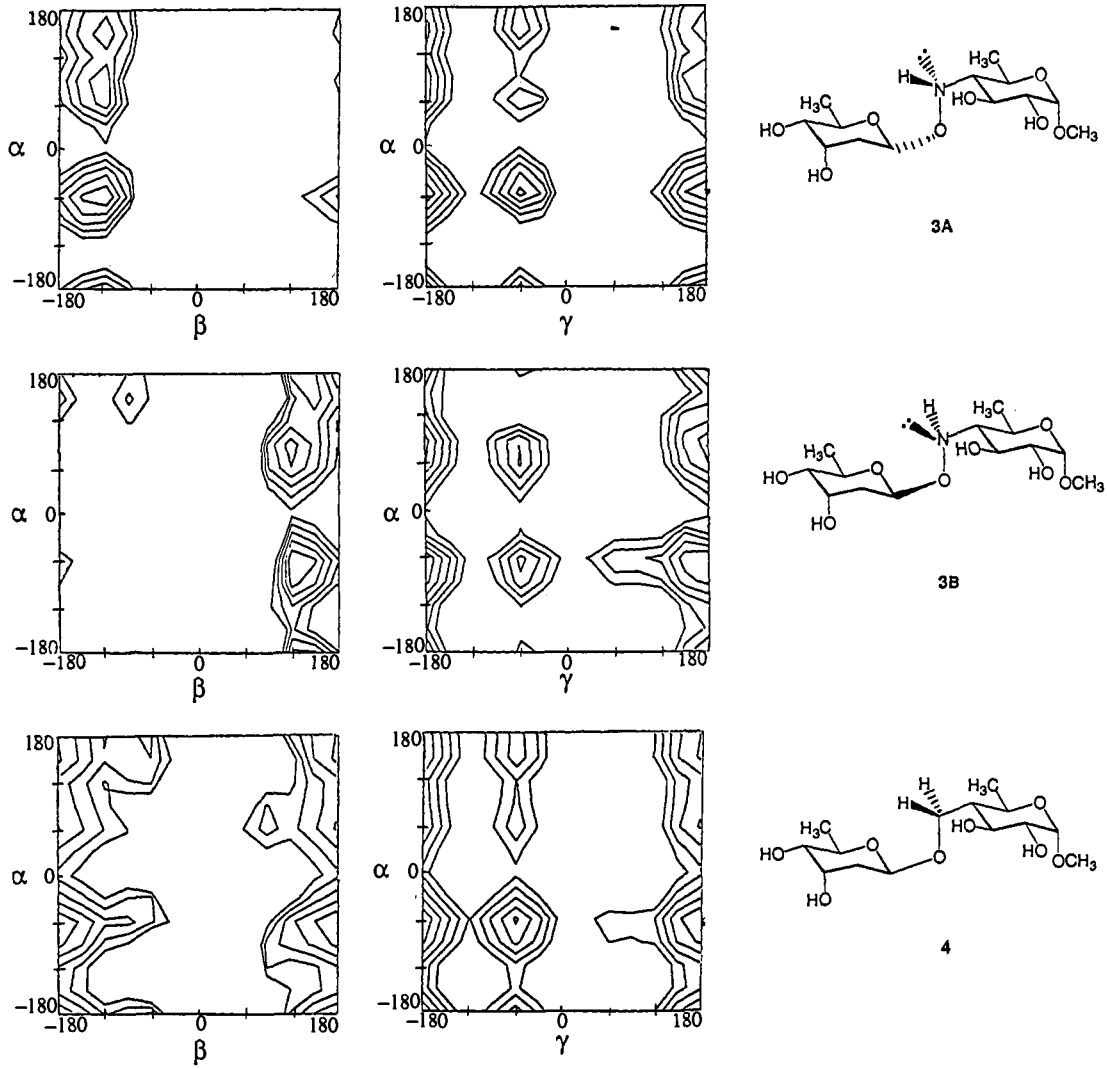


Figure 7. Contour plots representing the potential energy surface for model disaccharides 3 and 4.

Table 4. Preferred Torsion Angles of Low-Energy Conformers 3A, 3B, and 4[a]

| 3A | | | | 3B | | | | 4 | | | |
|---|---|---|---|---|---|---|---|---|---|---|---|
| $\Delta H$ | $\alpha$ | $\beta$ | $\gamma$ | $\Delta H$ | $\alpha$ | $\beta$ | $\gamma$ | $\Delta H$ | $\alpha$ | $\beta$ | $\gamma$ |
| 0.000 | -60.1 | -126.8 | 173.6 | 0.000 | -68.3 | 128.8 | 171.4 | 0.000 | -67.4 | 179.8 | 174.5 |
| 0.803 | 77.0 | -124.4 | 171.6 | 1.095 | 81.8 | 117.1 | 174.5 | 1.904 | 68.7 | -177.8 | 174.6 |
| 1.278 | 159.3 | -122.8 | 172.6 | 1.686 | 169.4 | 139.7 | 177.9 | 0.624 | 163.4 | 177.7 | 174.2 |
| 0.387 | -56.3 | -128.8 | -57.2 | 0.960 | -65.5 | 136.8 | -58.6 | 0.871 | -66.7 | -175.0 | -59.0 |
| 2.857 | 67.1 | -130.5 | -63.4 | 2.263 | 74.9 | 122.2 | -61.0 | 3.358 | 66.5 | -174.8 | -59.8 |
| 1.982 | 160.3 | -114.6 | -58.8 | 3.191 | 165.6 | 151.6 | -56.7 | 2.187 | 164.0 | -177.4 | -59.16 |

[a] $\Delta H$ in kcal/mol. $\alpha$, $\beta$, and $\gamma$ in degrees.

and the CO-containing disaccharide lie almost entirely in the $\beta$ angle. As shown below, the unusual torsion angle around the $\beta$ bond in the calicheamicin oligosaccharide has a profound effect on the overall shape of the molecule. The unusual shape conferred by the NO bond in calicheamicin appears to be critical for DNA binding (*vide infra*).

**Experimental Data on Disaccharides and Larger Systems.** There is a crystal structure reported for a calicheamicin derivative containing the hydroxylamine glycosidic linkage.[27] In this crystal structure, the $\alpha$, $\beta$, and $\gamma$ angles are -58.3°, -134.8°, and 167.0°, respectively, very close to those of the global minimum conformer calculated for disaccharide 3A ($\alpha$, $\beta$, and $\gamma$ = -60.1°, -126.8°, and 173.6°, respectively). The crystal structure thus confirms the eclipsed conformation around the NO bond as well as the -60° torsion predicted for the $\alpha$ angle and the (approximately) 170° torsion predicted for the $\gamma$ angle. NMR coupling constants (see Experimental Section) for the CO disaccharide also show that the torsion around the $\alpha$ angle in the CO disaccharide is approximately -60° (*i.e.*, both methylene hydrogens are gauche to the C4 hydrogen). Thus, the combined experimental data indicate that the conformation in which the C4 hydrogen and the glycosidic oxygen are anti to one another is heavily preferred for both the NO- and the CO-containing saccharides, consistent with the lowest energy $\alpha$ torsion identified from the calculations.[26] The secondary minima at $\alpha$ = 60° and 160° do not appear to be populated in solution. It is more difficult to establish definitively whether one or both predicted minima for the $\gamma$ angle are present in solution. Nevertheless, the $\gamma$ torsion in the crystal structure is consistent with the calculated global minimum $\gamma$ torsion for all three conformers, suggesting that it is indeed the global minimum.

(27) Lee, M. D.; Dunne, T. S.; Chang, C. C.; Ellestad, G. A.; Siegel, M. M.; Morton, G. O.; McGahren, W. J.; Borders, D. B. *J. Am. Chem. Soc.* **1987**, *109*, 3466.

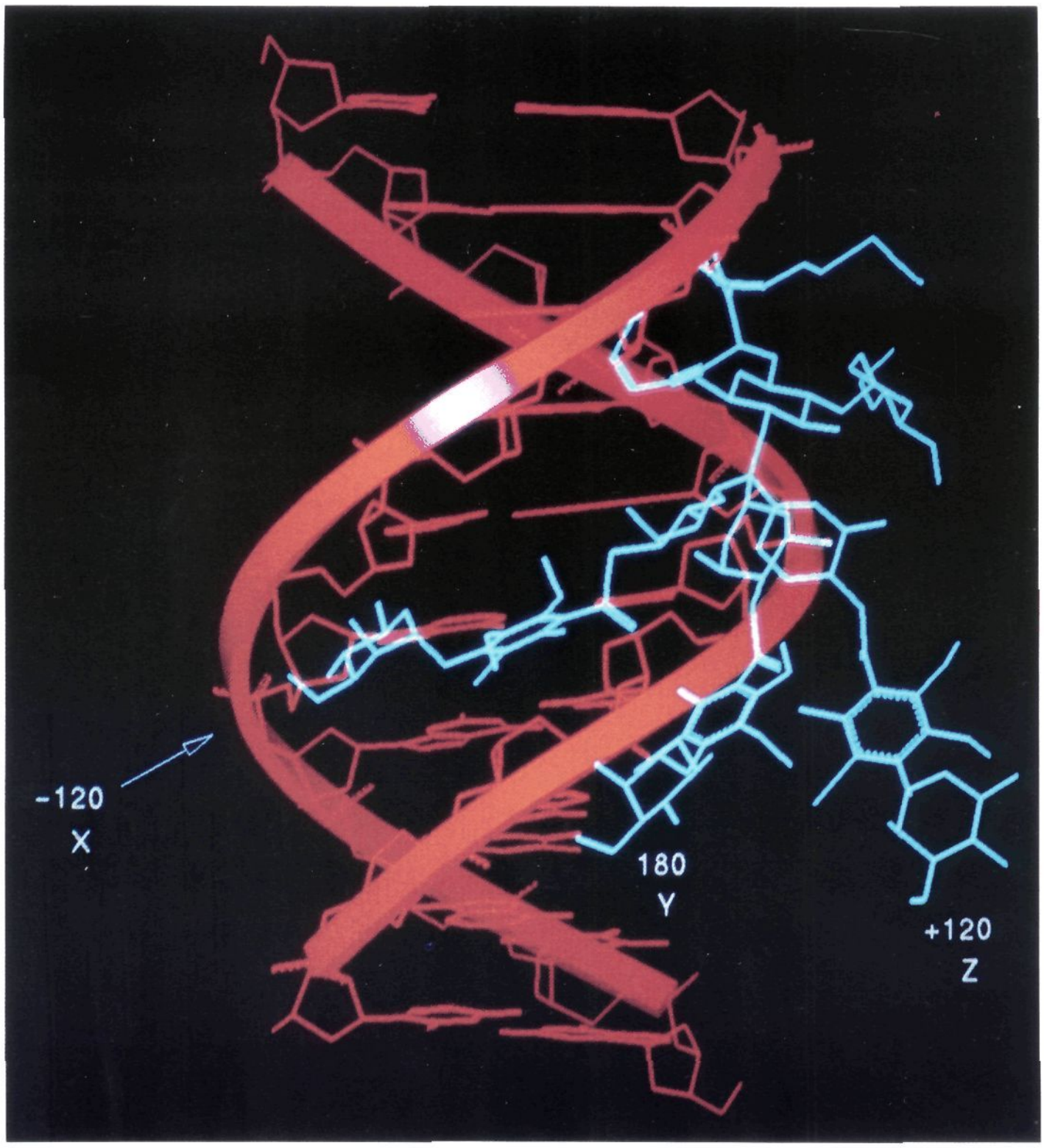


**Figure 8.** Molecular graphics model of two different N–O bond conformers (**X** and **Z**) and the C–O analogue (**Y**) of calicheamicin $\gamma^1$ docked into the minor groove of B-form DNA. The aglycone and the A and E rings have been superimposed. The orientation of the superimposed aglycones relative to the A and E rings is consistent with the experimental data on the structure of calicheamicin. The position of the aglycone in the groove is consistent with the experimental data on hydrogen atom abstraction and information on the structure of the calicheamicin–DNA complex. As the model shows, only structure **X** has a shape complementary to the groove. The structures **X** and **Z** do not contact the DNA distal to the A ring.

The fit between the hydroxylamine glycosidic linkage conformation in the crystal structure and that predicted for the NO disaccharide **3A** helps confirm the force field parametrization. However, the crystal structure provides only a static picture of the conformation around the hydroxylamine glycosidic linkage. The calculations suggest that the global minimum conformers for nitrogen invertomers **3A** and **3B** are very close in energy. To determine whether *both* nitrogen invertomers are likely to be present in solution, variable temperature experiments were performed on an NO disaccharide model system (**5**, see Experimental Section).[28] As with the monosaccharide, two sets of proton resonances were frozen out at low temperature (not shown). The population ratio was approximately 6:1, indicating that the energy difference between the conformers is larger in the disaccharide than in the monosaccharide. Assuming the NO disaccharide is a good model system for the hydroxylamine glycosidic linkage in calicheamicin itself, we conclude that at room temperature the calicheamicin oligosaccharide interconverts between a major and a minor nitrogen invertomer. In the calicheamicin oligosaccharide in solution, there is an NOE crosspeak between the B1 anomeric proton and the A6 methyl group. This NOE is consistent with the hydroxylamine glycosidic linkage isomer observed in the crystal structure but not with the other hydroxylamine glycosidic linkage isomer identified from the calculations. This NOE thus suggests that the major nitrogen invertomer in solution has a conformation similar to that of the crystal structure, with a $\beta$ torsion of approximately $-120°$.[29]

**Structural Consequences of the NO Bond and Implications for DNA Binding.** Both the force field calculations and the experimental data show that the NO bond enforces an unusual eclipsed conformation between the A and B sugars in the center of the calicheamicin oligosaccharide. To illustrate the profound influence this one bond can have on the overall shape of the molecule, we have generated models of both nitrogen invertomers of the

(28) The fully deprotected disaccharide on which the calculations were run is not soluble at low temperature. The NO disaccharide model system used in the dynamic NMR experiments, which has a benzyl ether at C2 of the A ring, may actually be a better model system for calicheamicin because the increased steric bulk at C2 is reminiscent of the E ring. Variable temperature experiments on calicheamicin itself were inconclusive because of resonance overlap and the complexity of the system, which prevented us from ascribing the observed line broadening to a specific process.[7]

(29) The relative size of the NOE crosspeak is smaller than expected.[24] This is consistent with the dynamic NMR experiments, which show that there are two interconverting NO bond isomers.

calicheamicin oligosaccharide and the CO analogue. These models, shown in Figure 8, differ *only* in the conformation around the $\beta$ angle. The $\beta$ angles for the three oligosaccharides are $-120°$, 180°, and $+120°$. The $\alpha$ and $\gamma$ angles for all three models are $-60°$ and 170°, consistent with the low-energy conformations for these bonds as determined from both calculations and the available experimental data. The torsion angles in the other interresidue linkages are identical in all three models and were adjusted to be consistent with experimental data on calicheamicin.[30] The models thus generated were overlaid so that the aglycone, A sugar and E sugar are superimposed. The superimposed aglycones were then docked into the minor groove of B-form DNA. The superimposed aglycones are oriented in the groove so that the carbons involved in radical abstraction are close to the ribose sugars on the opposite strands. As the figure illustrates, the $\beta$ torsion angle differences lead to dramatic differences in the overall shapes of the three molecules. Shape complementarity obviously plays a key role in binding affinity and selectivity. The structure with the $\beta$ torsion angle of $-120°$ (Figure 8, **X**) is the only one of the three structures with a curvature that is clearly complementary to the shape of the groove. When the aglycone is docked into the DNA in an orientation appropriate for radical abstraction from both DNA strands, the oligosaccharide tail of structure **X** winds around and down to follow the track of the minor groove. The other two structures do not even contact the groove distal to the A sugar of the oligosaccharide.

It should be noted that the conformation of the hydroxylamine glycosidic linkage in structure **X** is essentially identical to that in the crystal structure of the fragment of calicheamicin. This structure was also identified from combined experimental data and calculations on model systems as the major hydroxylamine isomer in solution.

We have recently reported the results of NMR studies on a calicheamicin–DNA complex which show that the oligosaccharide tail of calicheamicin binds in the minor groove at the pyrimidine recognition sequence.[5] In the bound oligosaccharide, there is a large intramolecular NOE between B1 and the A6 methyl. This NOE is consistent with the $-120°$ hydroxylamine glycosidic linkage conformer in structure **X** (Figure 8). Moreover, several intermolecular NOEs between the oligosaccharide and the DNA indicate that the relative orientation of the A and B sugars in the minor groove must be similar to that shown in structure **X**. Therefore, we have concluded that the conformation of the bound oligosaccharide resembles structure **X** (Figure 8), which we think is the lowest energy conformation in solution (and which is also the conformation seen in the crystal structure, *vide supra*). Thus, as Figure 8 should make clear, the hydroxylamine bond plays a major role in organizing the calicheamicin molecule into a shape suitable for minor groove binding.

(30) NOE data on calicheamicin in solution and bound to DNA have been found to be consistent with the NMR data and with the crystal structure.

## Summary and Conclusion

We have developed parameters for hydroxylamine glycosidic linkages for use with the AMBER force field and have established the validity of the parametrization using experimental data. We have used a combination of the experiments and force field calculations to identify the low-energy conformations around the hydroxylamine glycosidic linkage in the calicheamicin oligosaccharide. We have shown that the major hydroxylamine conformer in solution has a shape complementary to the shape of the minor groove. Previously reported NMR data on a calicheamicin–DNA complex indicate that the major hydroxylamine conformer in solution is, in fact, the conformer that binds to DNA.

Our analysis suggests that the peculiar hydroxylamine glycosidic linkage in calicheamicin, with its distinctive torsion angle preferences, is a design element used by nature to construct an oligosaccharide with the appropriate shape (and rigidity) to bind selectively in the minor groove of DNA. It is difficult to imagine another bond that could substitute for this linkage and still preserve the appropriate spatial orientation of the two halves of the molecule. We hope that a combination of experimental NMR data on the calicheamicin–DNA complex and force field calculations using the newly parametrized AMBER force field contained within DISCOVER will shed further light on the molecular basis for selective binding of calicheamicin to pyrimidine runs of DNA.

**Acknowledgment.** This work was supported by the National Institutes of Health.